Scientific Report

TRANSPARENT PROCESS

EMBO reports

Genome-wide screen identifies signaling pathways that regulate autophagy during *Caenorhabditis elegans* development

Bin Guo[1,2,3,†], Xinxin Huang[3,†], Peipei Zhang[2], Linxiang Qi[2], Qianqian Liang[2], Xuebo Zhang[3], Jie Huang[2], Bin Fang[2], Wenru Hou[2], Jinghua Han[2] & Hong Zhang[2,*]

Abstract

The mechanisms that coordinate the regulation of autophagy with developmental signaling during multicellular organism development remain largely unknown. Here, we show that impaired function of ribosomal protein RPL-43 causes an accumulation of SQST-1 aggregates in the larval intestine, which are removed upon autophagy induction. Using this model to screen for autophagy regulators, we identify 139 genes that promote autophagy activity upon inactivation. Various signaling pathways, including Sma/Mab TGF-β signaling, *lin-35*/Rb signaling, the XBP-1-mediated ER stress response, and the ATFS-1-mediated mitochondrial stress response, regulate the expression of autophagy genes independently of the TFEB homolog HLH-30. Our study thus provides a framework for understanding the role of signaling pathways in regulating autophagy under physiological conditions.

Keywords autophagy; *Caenorhabditis elegans*; ER stress; mitochondrial stress; Rb

Subject Categories Autophagy & Cell Death; Signal Transduction; Membrane & Intracellular Transport

DOI 10.1002/embr.201338310 | Received 4 December 2013 | Revised 27 March 2014 | Accepted 28 March 2014 | Published online 24 April 2014

EMBO Reports (2014) 15, 705–713

Introduction

Autophagy is an evolutionarily conserved lysosome-mediated degradation process. It involves the formation of a cup-shaped membrane sac, known as the isolation membrane, which expands and seals to form an enclosed double-membrane autophagosome. In higher eukaryotes, autophagosomes mature by fusing with endosomes before fusing with lysosomes to form degradative autolysosomes [1–3]. Distinct steps of autophagosome formation require different sets of genes [2,4]. The Atg1/Atg13 kinase complex and the Vps34/Atg6 class III PI(3)K complex are required for the induction and nucleation of isolation membranes. Expansion and closure of the autophagosome is regulated by the Atg8-phosphatidylethanolamine (PE) and Atg12-Atg5 ubiquitin-like conjugation systems [2]. Progression of autophagosomes into autolysosomes requires components of the endocytic pathways and the SNARE complex [3,5].

Autophagy is activated by a variety of stress conditions, including nutrient starvation, energy deprivation, and reactive oxygen species [6]. The mammalian target of rapamycin serine/threonine kinase complex 1 (mTORC1) and the Vps34 PI(3)K complex are major nodes for integrating various signaling pathways with autophagy regulation [7–9]. Transcriptional regulation of autophagy genes confers another layer of regulation. The master positive regulator TFEB and the master repressor ZKSCAN3 transcriptionally regulate a network of genes involved in autophagosome and lysosome biogenesis [10,11]. The forkhead transcription factor FoxO also activates the transcription of multiple autophagy genes and promotes autophagy activity [6]. Although numerous factors have been uncovered that regulate autophagy activity, the mechanisms that integrate developmental signals into the autophagic machinery during multicellular organism development are poorly understood.

Here, we established *Caenorhabditis elegans* as a genetic model to study autophagy regulation and identified 139 genes which, when inactivated, enhance autophagy activity. We showed that autophagy activity is activated by various stress-induced conditions and is tightly controlled by various developmental signaling pathways.

Results and Discussion

Loss of *rpl-43* activity results in accumulation of SQST-1 aggregates in the larval intestine

The *C. elegans* p62 homolog SQST-1 is removed by autophagy during development. In wild-type animals, SQST-1::GFP is weakly and diffusely expressed in the cytoplasm from embryonic to adult

1 College of Life Sciences, China Agricultural University, Beijing, China
2 State Key Laboratory of Biomacromolecules, Institute of Biophysics, Chinese Academy of Sciences, Beijing, China
3 National Institute of Biological Sciences, Beijing, China
*Corresponding author. Tel: +86 10 64848238; Fax: +86 10 64853925; E-mail: hongzhang@sun5.ibp.ac.cn
†These authors contributed equally to this manuscript.

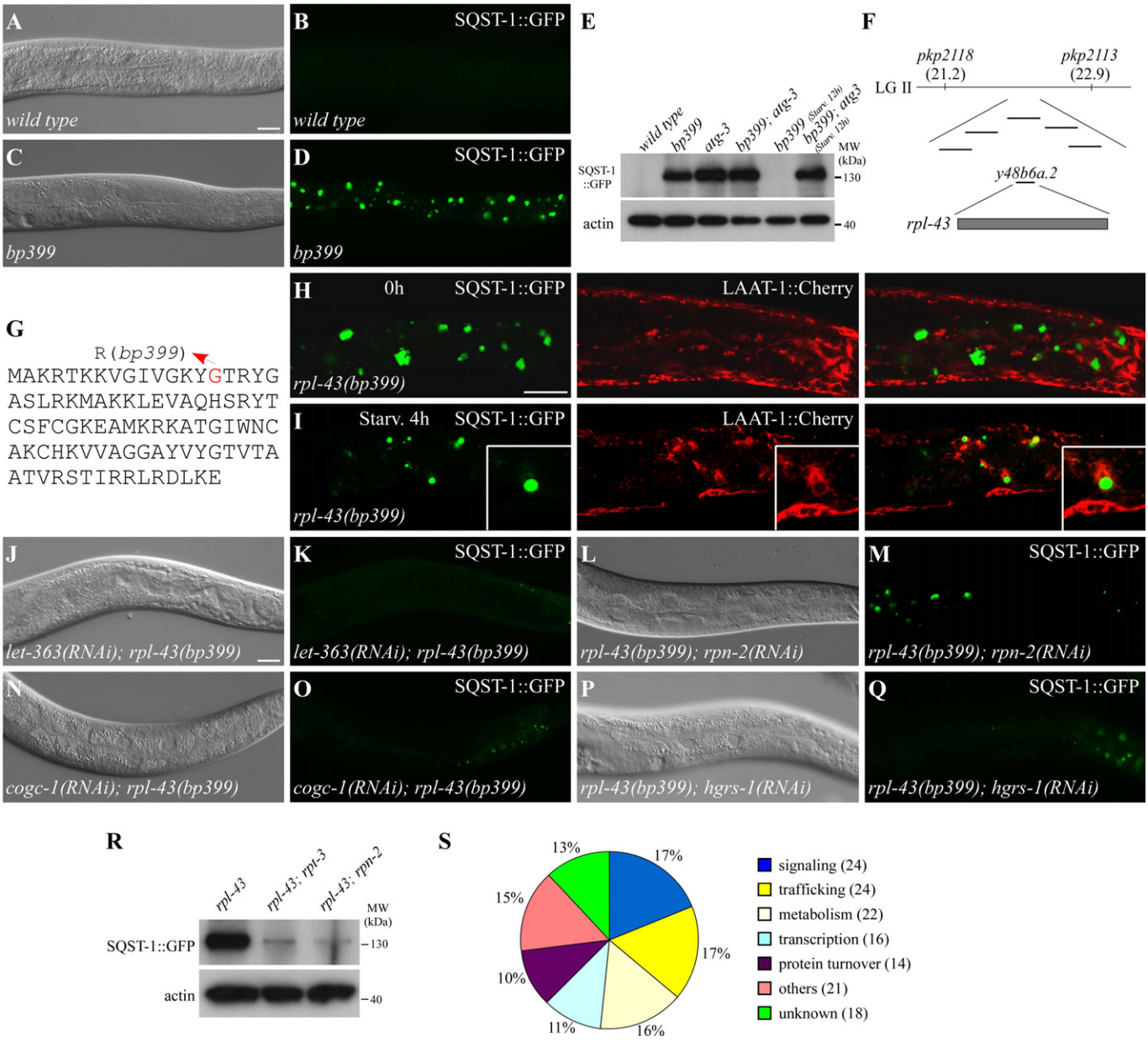

Figure 1. Genome-wide RNAi screen for gene inactivations that suppress the accumulation of SQST-1::GFP aggregates in *rpl-43* mutants.

A–D SQST-1::GFP is very weakly expressed and diffusely localized in the cytoplasm in wild-type larval intestine, but is expressed at much higher levels and accumulates into numerous aggregates in the intestine in *bp399* mutant larvae. (A) and (C) represent DIC images of the animals in (B) and (D), respectively.

E Compared to wild-type, SQST-1::GFP levels are much higher in *bp399* and *bp412* mutant larvae as shown by immunoblotting assay. SQST-1::GFP levels in *bp399* mutants are greatly reduced after 12 h of starvation. 200 young adult animals for each genotype were collected for analysis.

F Mapping and cloning of *bp399*. LG II: linkage group II.

G Protein sequence of RPL-43. The mutated residue in *bp399* is highlighted in red.

H, I SQST-1::GFP aggregates in *rpl-43*(*bp399*) mutants are separable from LAAT-1::Cherry-labeled lysosomes under normal conditions, but are delivered to lysosomes upon starvation. Some aggregates are enclosed by lysosomes (inserts). Scale bar: 20 μm.

J–Q RNAi inactivation of *let-363*, *rpn-2*, *cogc-1*, or *hgrs-1* suppresses the accumulation of SQST-1::GFP aggregates in *rpl-43*(*bp399*) mutants. (J), (L), (N), and (P): DIC images of the animals in (K), (M), (O), and (Q). Scale bar: 20 μm.

R SQST-1::GFP levels in *rpl-43*(*bp399*) mutants are greatly reduced by inactivation of *rpt-3* and *rpn-2*. 200 young adult animals for each genotype were collected for analysis.

S Functional classification of the identified genes. The number of genes in each functional class is shown in parentheses.

stages (Fig 1A and B; Supplementary Fig S1A and B) [12]. In autophagy mutants, numerous SQST-1::GFP aggregates accumulate in almost all cells during embryogenesis and in multiple larval tissues, including hypodermis, intestine, and neurons (Supplementary Fig S1C and E–L). Intestinal SQST-1 aggregates, which are spherical and dispersed in the cytoplasm, accumulate throughout larval

stages in autophagy mutants (Supplementary Fig S1E–L). *bp399* was isolated in a genetic screen for mutants with defective degradation of SQST-1::GFP (Fig 1C–E). Unlike autophagy mutants, *bp399* mutants showed the accumulation of SQST-1 aggregates strictly in the intestine in a distinct temporal pattern. SQST-1::GFP aggregates were absent in *bp399* embryos, but started to form in L1 larvae and increased in number and size throughout larval development (Fig 1C and D; Supplementary Fig S1D and M–T). SQST-1::GFP aggregates in *bp399* were heterogeneous in size and some were much larger than those in autophagy mutants (Supplementary Fig S1E–T). Endogenous SQST-1 also accumulated in the intestine in *bp399* mutants (Supplementary Fig S1U–X). SQST-1::GFP aggregates in *bp399* mutants were co-stained by anti-ubiquitin, suggesting the accumulation of ubiquitinated proteins (Supplementary Fig S1Y–B2).

A transgene containing the single gene *rpl-43* rescued the SQST-1::GFP accumulation phenotype in *bp399* mutants (Fig 1F). The glycine at position 15 of RPL-43 was mutated to arginine in *bp399* mutants (Fig 1G). *rpl-43* encodes the 60S ribosomal protein L37. RNAi inactivation of other ribosomal subunits, ribosomal maturation factors, and translation initiation factors resulted in the same phenotype as *rpl-43*(*bp399*) (Supplementary Table S1; Supplementary Fig S1C2–F2). This suggests that impaired protein synthesis causes the accumulation of SQST-1 aggregates in the larval intestine.

Autophagic degradation of other autophagy substrates was unaffected in *rpl-43* mutants (Supplementary Fig S2A–P) [13]. Levels of the *C. elegans* Atg8 homolog LGG-1, which has been widely used to measure autophagy activity, were unaltered in *rpl-43* mutants and no intestinal LGG-1 puncta were detected (Supplementary Fig S2Q–T). Thus, *rpl-43* is not an essential component of the autophagy pathway.

SQST-1 aggregates in *rpl-43* mutants are degraded by elevated autophagy activity

Starvation or inactivation of Tor signaling resulted in the degradation of SQST-1 aggregates in *rpl-43* mutants, but not in autophagy mutants (Fig 1E, J, and K; Supplementary Fig S3A–N). Intestinal SQST-1 aggregates persisted in *rpl-43; atg-3* mutants after starvation or *let-363/mTOR* inactivation (Supplementary Fig S3O and P). We then followed the dynamic distribution of SQST-1::GFP aggregates and lysosomes. SQST-1::GFP aggregates and LAAT-1::cherry-labeled lysosomes were separable in *rpl-43* mutants (Fig 1H). Upon starvation, SQST-1::GFP aggregates in *rpl-43* mutants fused and became encircled by lysosomes (Fig 1I). Thus, the SQST-1 aggregates in *rpl-43* mutants are degraded upon autophagy induction.

Genome-wide RNAi screen for gene inactivation elevating autophagy activity

We screened a *C. elegans* RNAi feeding library targeting 16,749 genes (~87% of *C. elegans* ORFs) to identify RNAi clones that significantly suppressed the SQST-1::GFP aggregate accumulation phenotype in *rpl-43* mutants (Fig 1L–R). The RNAi clones that reproducibly suppressed *rpl-43* were subjected to several additional screens. First, a *GFP* reporter driven by the *sqst-1* promoter was screened to exclude genes that transcriptionally repress *sqst-1* (Supplementary Fig S3Q–T). Second, to exclude RNAi inactivations that cause disappearance of SQST-1 aggregates by mechanisms independent of autophagy induction, we screened for RNAi clones that did not affect the accumulation of intestinal SQST-1 aggregates in *atg-9* mutants. Third, we identified gene inactivations that promoted the degradation of another autophagy substrate W07G4.5::GFP in the intestine (Supplementary Fig S3U–X) [14]. After these screens, 139 genes were identified as suppressors of *rpl-43* (Table 1; Supplementary Table S2).

Based on annotated biological function, the 139 genes were enriched for signal transduction, protein turnover, intracellular trafficking, and cellular metabolism processes (Fig 1S). According to gene ontology, 111 of the genes have clear human homologs.

We identified genes encoding proteins involved in the ubiquitin-proteasome degradation system (UPS), including components of the proteasome and the Cdc48/Ufd1/Npl4 complex involved in ER-associated degradation (ERAD), and also genes encoding transcription factors, metabolic enzymes, and transporters (Table 1; Fig 1L, M, and R). Genes encoding factors involved in intracellular trafficking included the central and lobe A subunits of the conserved oligomeric Golgi (COG) complex, clathrin adaptor protein complex AP-2, and components of the endosomal sorting ESCRT complex (Fig 1N–Q). Our screen identified genes involved in developmental signaling pathways, including TGF-β signaling (*sma-3, sma-4*), Hippo signaling (*wts-1*), PKC1-MPK1 signaling (*gls-1*), Notch signaling (*glp-1*), and the ERK MAPK pathway (*mek-2*).

Genome-wide functional interaction maps have been created for *C. elegans* based on gene expression, physical and genetic interactions, and functional annotation [15,16]. Among the 139 genes, 72 genes (nodes) formed at least one interaction (edge) with other genes, and a total of 103 edges were identified (Supplementary Fig S3Y). As a control, we randomly selected four groups of 139 genes from the same library, which showed 3, 0, 4, and 5 interactions, respectively.

Sma TGF-β signaling regulates autophagy

The Sma/Mab and Dauer TGF-β signaling pathways in *C. elegans*, consisting of distinct components, regulate different developmental processes (Supplementary Fig S4A) [17]. In addition to *sma-3* and *sma-4* (Smads) identified in our screen (Fig 2A–D), knockdown of other components in the Sma TGF-β pathway, including *dbl-1* (ligand), *sma-6* (type I receptor), *sma-2* (Smad), and *sma-9* (cofactor), also suppressed SQST-1 aggregates in *rpl-43* mutants (Supplementary Fig S4B). Inactivation of Sma/Mab TGF-β signaling suppresses the *rpl-43* mutant phenotype independent of its role in regulating body size (Supplementary Fig S4B–D). Loss of function of components in the Dauer TGF-β signaling pathway, including *daf-7* (ligand), *daf-1* (type I receptor), *daf-8* (Smad), and *daf-3* (Smad), did not suppress SQST-1 aggregates in *rpl-43* mutants (Supplementary Fig S4B, E and F).

Expression of endogenous LGG-1 and GFP::LGG-1 was greatly increased and a large number of GFP::LGG-1 puncta formed in *dbl-1* and *sma-3* mutants compared to wild-type animals (Fig 2E; Supplementary Fig S4G and H). mRNA levels of *lgg-1* and other autophagy genes, including *bec-1*, *epg-8*, and *atg-7*, were increased in *dbl-1*, *sma-2*, and *sma-3* mutants (Fig 2F), indicating that Sma TGF-β signaling regulates autophagy at least partially through transcriptional control of autophagy genes.

Table 1. List of some RNAi inactivations that lead to suppression of the accumulation of SQST-1::GFP aggregates in the intestine in *rpl-43* mutants

Process	Sequence name	Gene name	Brief description of gene product
Signaling	F54C8.5	*rheb-1*	Orthologous to the mammalian Rheb and Rheb1 GTPases
Signaling	R13F6.9	*sma-3*	A Smad protein
Signaling	R12B2.1	*sma-4*	A Smad protein
Signaling	F02A9.6	*glp-1*	N-glycosylated transmembrane protein
Signaling	T20F10.1	*wts-1*	Warts/lats-like serine threonine kinase
Signaling	F42G8.8		Serine/threonine-protein phosphatase PP1
Signaling	C36B1.8	*gls-1*	Transducer of the stress-activated PKC1-MPK1 signaling pathway
Signaling	Y54E10BL.6	*mek-2*	Mitogen-activated protein kinase kinase
Protein turnover	F23F12.6	*rpt-3*	An AAA ATPase subunit of the 19S regulatory particle of the 26S proteasome
Protein turnover	F19B6.2	*ufd-1*	Protein involved in the recognition of polyubiquitinated proteins
Protein turnover	F59E12.5	*npl-4.2*	Ubiquitin-binding protein involved in protein degradation
Protein turnover	C06A1.1	*cdc-48.1*	An AAA ATPase homologous to yeast Cdc48 and mammalian p97/VCP
Transcription	F47D12.4	*hmg-1.2*	HMG box-containing protein
Transcription	F31E3.1	*ceh-20*	Homeobox family member
Transcription	C01B7.1	*ztf-12*	Zinc finger transcription factor family
Transcription	R06C7.7	*lin-61*	Polycomb group protein SCM/L(3)MBT
Transcription	C32F10.2	*lin-35*	The *Caenorhabditis elegans* retinoblastoma protein (Rb) ortholog
Transcription	JC8.6	*lin-54*	Metallothionein-like protein
Transcription	F52C12.5	*elt-6*	GATA-4/5/6 transcription factor
Transcription	F44C4.2	*nhr-37*	Nuclear hormone receptor
Transcription	D2021.1	*utx-1*	General transcriptional co-repressor
Transcription	C33D3.1	*elt-2*	GATA-type transcription factor
Protein trafficking	C07G1.5	*hgrs-1*	Membrane trafficking and cell signaling protein HRS
Protein trafficking	ZK652.2	*tomm-7*	Translocase of outer mitochondrial membrane complex
Protein trafficking	E04A4.5		Mitochondrial import inner membrane translocase
Protein trafficking	F35H10.4	*vha-5*	Subunit a of the vacuolar H + -ATPase V0 sector
Protein trafficking	CD4.4	*vps-37*	A member of the endosomal sorting ESCRT-I complex
Metabolism	F54D8.3	*alh-1*	Aldehyde dehydrogenase
Metabolism	C28H8.11		Tryptophan 2,3-dioxygenase
Metabolism	F37E3.1	*ncbp-1*	Nuclear cap-binding protein complex
Metabolism	K04E7.2	*pep-2*	A low-affinity/high-capacity oligopeptide transporter

The LIN-35/Rb pathway regulates autophagy

Our screen identified several class B synthetic multivulva (SynMuvB) genes, including *lin-35* (the Rb homolog), *lin-54,* and *lin-61* (Fig 2C, D, G, and H; Supplementary Fig S5A–D). Endogenous SQST-1 aggregates were absent in *rpl-43; lin-35* mutants (Supplementary Fig S5E and F). SynMuvB genes function redundantly with class A or class C SynMuv genes to antagonize specification of the vulva cell lineage [18]. RNAi knockdown of other SynMuvB genes, including *lin-15B* and *lin-36*, components of a Rb-containing DRM complex (*dpl-1*, *lin-9*, *lin-37*, *lin-53*), a SynMuvB heterochromatin complex (*hpl-2*, *lin-13*), and a SUMO-recruited Mec complex (*mep-1* and *let-418*), all suppressed the accumulation of SQST-1::GFP aggregates in *rpl-43* mutants (Supplementary Fig S5G). However, RNAi inactivation of class A (*lin-15A*, *lin-8,* and *lin-56*) and class C (*trr-1* and *mys-1*) SynMuv genes had no effect (Fig 2I and J; Supplementary Fig S5G). Knockdown of genes essential for SynMuvB function in vulval development, RNAi, and soma-germ fate determination did not cause reappearance of SQST-1 aggregates in *lin-35; rpl-43* mutants (Supplementary Fig S5H–M). Thus, SynMuvB genes regulate autophagy activity independent of their role in other processes.

The number of GFP::LGG-1 puncta and levels of endogenous LGG-1 were dramatically elevated in *lin-35*, *lin-15B,* and *lin-9* mutants (Fig 2K; Supplementary Fig S5N and O). Levels of *bec-1*, *epg-8*, *lgg-1,* and *atg-7* mRNA were increased in *lin-35*, *lin-15B*, *lin-9,* and *mep-1* mutants (Fig 2L and data not shown). Thus, the *lin-35*/Rb pathway transcriptionally regulates autophagy genes.

daf-2 insulin/IGF signaling regulates autophagy activity

Reduction of *daf-2* signaling elevates autophagy activity [19]. Accumulation of SQST-1 aggregates in *rpl-43* mutants was

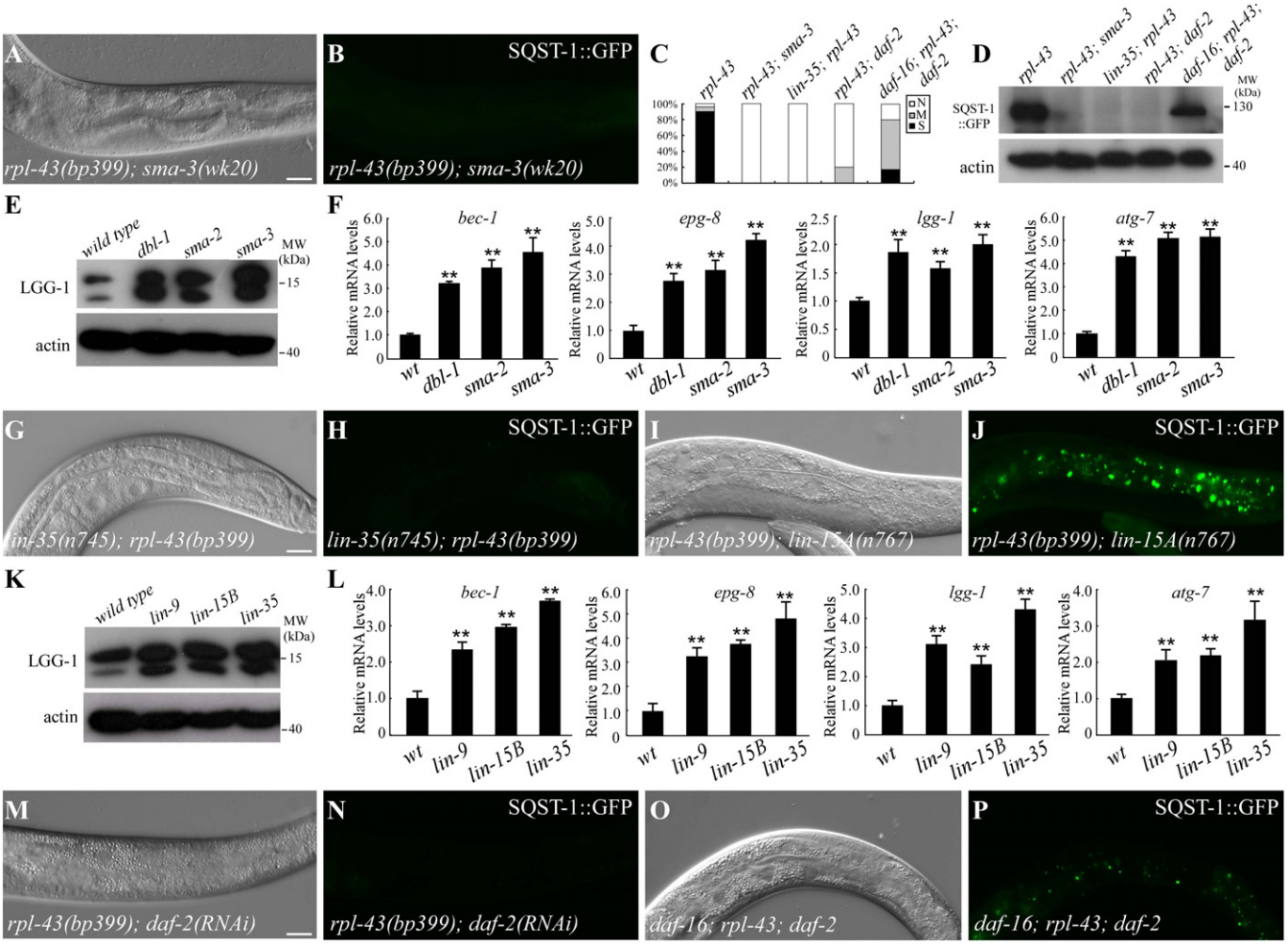

Figure 2. Loss of function of a variety of signaling pathways suppresses the *rpl-43* phenotype.

A, B SQST-1::GFP aggregates are absent in the *rpl-43*(*bp399*); *sma-3*(*wk20*) mutant intestine.

C Percentage of the indicated animals with different levels of SQST-1::GFP aggregates. S: many SQST-1::GFP aggregates in all intestinal cells, as in *rpl-43*(*bp399*) mutants; M: fewer SQST-1::GFP aggregates in some but not all intestinal cells; N: no or very few SQST-1::GFP aggregates in intestinal cells. For each genotype, > 30 animals were examined.

D SQST-1::GFP levels in *rpl-43*(*bp399*) mutants are dramatically decreased in a Western blot when *sma-3*, *lin-35*, or *daf-2* is simultaneously depleted. Loss of function of *daf-16* partially restores SQST-1 levels in *rpl-43*(*bp399*); *daf-2*(*RNAi*) mutants.

E Endogenous LGG-1 is elevated in a Western blot in *dbl-1*(*wk70*), *sma-2*(*e502*), and *sma-3*(*wk20*) mutants.

F mRNA levels of *bec-1*, *epg-8*, *lgg-1*, and *atg-7* are upregulated in *dbl-1*(*wk70*), *sma-2*(*e502*), and *sma-3*(*wk20*) mutants. $^{**}P < 0.01$. 500 young adult animals were collected for analysis. Error bars indicate s.d. from three experiments.

G, H No SQST-1::GFP aggregates are observed in the *lin-35*(*n745*); *rpl-43*(*bp399*) mutant intestine.

I, J Numerous SQST-1::GFP aggregates are formed in *rpl-43*(*bp399*); *lin-15A*(*n767*) mutants.

K Endogenous LGG-1 levels are increased in *lin-9*(*n112*), *lin-15B*(*n744*), and *lin-35*(*n745*) mutants.

L mRNA levels of *bec-1*, *epg-8*, *lgg-1*, and *atg-7* are upregulated in *lin-9*(*n112*), *lin-15B*(*n744*), and *lin-35*(*n745*) mutants. $^{**}P < 0.01$. 500 young adult animals were collected for analysis. Error bars indicate s.d. from three experiments.

M, N *rpl-43*(*bp399*); *daf-2*(*RNAi*) mutant larvae contain no intestinal SQST-1::GFP aggregates.

O, P SQST-1::GFP aggregates are partially restored in *daf-16*(*mu86*); *rpl-43*(*bp399*); *daf-2*(*RNAi*) animals.

Data information: 200 young adult animals for each genotype were collected for analysis in (D), (E), and (K). Scale bars: 20 μm (A, B, G–J, M–P). (A), (G), (I), (M), and (O): DIC images of the animals in (B), (H), (J), (N), and (P), respectively.

suppressed by the loss of function of *daf-2* and *pdk-1* (Fig 2C, D, M, and N; Supplementary Fig S6A and B). Reduced *daf-2* activity results in nuclear translocation of the forkhead transcription factor DAF-16, which further activates the expression of downstream target genes. SQST-1 aggregates were partially restored in *daf-16; rpl-43; daf-2* mutants (Fig 2C, D, O, and P), indicating that *daf-2* regulates autophagy activity partially through DAF-16. *daf-16* is not required for suppression of *rpl-43* by inactivation of *let-363*, *sma-3*, and *lin-35* (Supplementary Fig S6C–H).

daf-2 mutants did not show elevated LGG-1 levels by immunoblotting (Supplementary Fig S6I). mRNA levels of *lgg-1*, but not of other autophagy genes, were slightly increased in *daf-2* mutants (Supplementary Fig S6J). Upregulation of *lgg-1* was suppressed by the loss of *daf-16* activity (Supplementary Fig S6J). DAF-16 negatively regulates *daf-15* transcription [20]. Knockdown of mTOR or raptor did not increase mRNA levels of autophagy genes (Supplementary Fig S6K). These results suggest that *daf-2* may regulate autophagy by converging on DAF-15, as in the regulation of dauer formation and fat accumulation [20].

ER stress activates autophagy activity

Accumulation of unfolded/misfolded proteins in the endoplasmic reticulum (ER) triggers the ER unfolded protein response (UPR) to ameliorate the stress [21]. *bp399* did not cause evident ER stress, as shown by very low expression of the ER stress marker P*hsp-4::GFP* (Fig 3A and B; Supplementary Fig S7A and B). Treatment of *rpl-43* mutants with tunicamycin and DTT induced ER stress and strongly suppressed the accumulation of SQST-1 aggregates (Fig 3C; Supplementary Fig S7E-H). P*hsp-4::GFP* expression was also greatly increased by RNAi inactivation of 24 genes identified in our screen, including components of the proteasome and the ERAD complex (Supplementary Table S3; Fig 3D and E; Supplementary Fig S7I and J). Among the 24 ER stress-inducing genes, 10 are functionally connected and share 19 interactions (edges) in total (Fig 3L).

In *C. elegans*, IRE-1-XBP-1, the PERK kinase homolog PEK-1, and activating transcription factor-6 (ATF-6) sense ER stress and activate the UPR. To determine whether UPR activation plays a causative role in autophagy induction, we examined the role of *xbp-1*, *pek-1*, and *atf-6* in suppression of the *rpl-43* phenotype by the 24 identified genes. Loss of activity of *ire-1*, *xbp-1*, *pek-1*, or *atf-6* had no evident effect on the expression of P*hsp-4::GFP* or the number of SQST-1 aggregates in *rpl-43* mutants (Supplementary Fig S7C, D, M, and N).

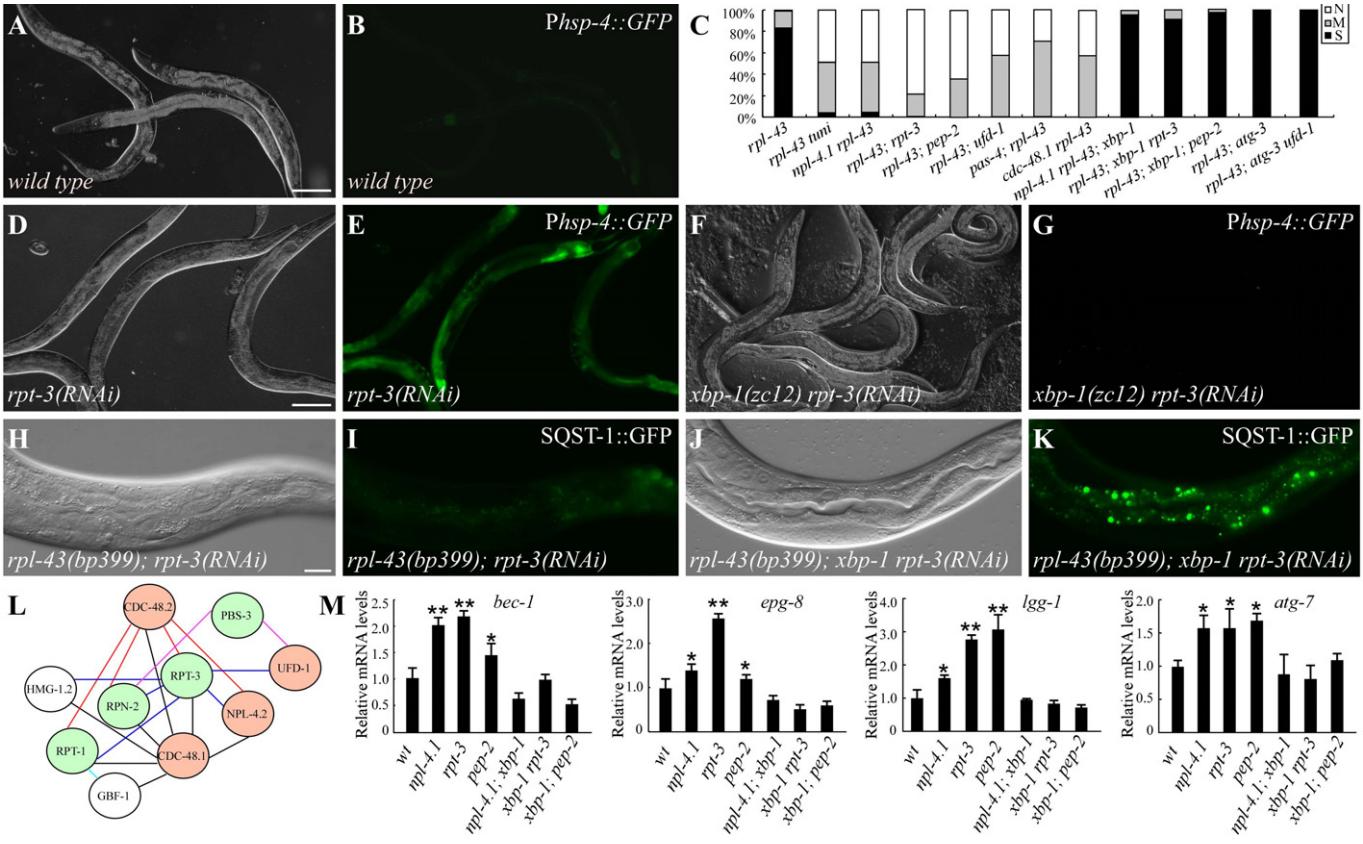

Figure 3. XBP-1-mediated ER stress suppresses the *rpl-43* phenotype.

A, B P*hsp-4::GFP* is very weakly expressed in wild-type animals.

C Percentage of indicated animals with different levels of SQST-1::GFP aggregates. S: strong. M: medium. N: none. >30 animals were examined for each genotype.

D, E P*hsp-4::GFP* expression is much higher in *rpt-3*(*RNAi*) animals.

F, G Upregulation of P*hsp-4::GFP* expression in *rpt-3*(*RNAi*) animals is suppressed by the *xbp-1*(*zc12*) mutation.

H, I SQST-1::GFP aggregates are absent in *rpl-43*(*bp399*); *rpt-3*(*RNAi*) animals.

J, K Loss of function of *xbp-1* restores SQST-1::GFP aggregates in *rpl-43*(*bp399*); *rpt-3*(*RNAi*) animals.

L Functional interaction of ER stress-induced genes.

M The increase in *bec-1*, *epg-8*, *lgg-1*, and *atg-7* mRNA levels in *npl-4.1*, *rpt-3*, and *pep-2* RNAi animals is dependent on *xbp-1*. *$P < 0.05$, **$P < 0.01$. 500 young adult animals were collected for analysis. Error bars indicate s.d. from three experiments.

Data information: (A), (D), (F), (H), and (J): DIC images of the animals in (B), (E), (G), (I), and (K), respectively. Scale bars: 100 μm (A, B, D–G); 20 μm (H–K).

Simultaneous inactivation of *xbp-1* blocked upregulation of P*hsp-4::GFP* in ER stress-induced mutant animals (Fig 3F and G; Supplementary Fig S7K and L). In *rpl-43; xbp-1* double mutants, SQST-1 aggregates persisted upon DTT treatment or knockdown of identified ER stress-induced genes except *unc-89* (Fig 3H–K; Supplementary Fig S7O-R). SQST-1::GFP aggregates were restored in *unc-89; rpl-43* mutants by *atf-6* inactivation (Supplementary Fig S7S–V). Inactivation of *pek-1* or *atf-6* did not affect other identified ER stress-induced genes. Thus, XBP-1 mediates the induction of autophagy by ER stress. SQST-1 aggregates in *rpl-43; xbp-1* mutants were still suppressed by the inactivation of TOR signaling, *daf-2*, *sma-3,* and *lin-35* (Supplementary Fig S7W–Z), indicating that impaired ER stress did not block autophagy induction by other signaling pathways.

We determined the expression of autophagy genes in ER stress-induced mutants. GFP::LGG-1 forms a large number of puncta in the intestine after knockdown of *ufd-1*, *npl-4.2,* and *pep-2* (Supplementary Fig S7A2 and B2). Levels of *bec-1*, *epg-8*, *lgg-1,* and *atg-7* mRNA were increased in *npl-4.1-*, *rpt-3-,* and *pep-2*-knockdown animals (Fig 3M). Simultaneously depleting *xbp-1* abolished the upregulation of autophagy genes in these same mutants (Fig 3M).

Mitochondrial stress upregulates autophagy activity

Perturbation of the protein-folding environment in the mitochondrial matrix activates the mitochondrial unfolded protein response (UPR^{mt}) to re-establish protein homeostasis [22]. Inactivation of *spg-7* (not included in the RNAi feeding library), encoding *C. elegans* paraplegin, induced mitochondrial stress and suppressed SQST-1::GFP aggregates in *rpl-43* mutants (Supplementary Fig S8A, B, J and K). RNAi inactivation of 6 genes identified in our screen, namely *egl-46*, *gfi-1, vha-15*, *tomm-7*, *tomm-22,* and *E04A4.5*, increased the expression of the mitochondrial stress marker P*hsp-60::GFP* (Fig 4A and B; Supplementary Fig S8C and D).

The bZip transcription factor ATFS-1 is essential for UPR^{mt} activation in *C. elegans* [22]. *atfs-1*(*RNAi*) suppressed the elevated expression of P*hsp-60::GFP* in *spg-7* and 6 other identified mutants and also rescued the suppression effect of SQST-1 aggregates in *rpl-43* mutants (Fig 4C-H; Supplementary Fig S8E-P). *atfs-1* is not required for the suppression effect caused by the loss of activity of *sma-3*, *lin-35,* and *daf-2* (Supplementary Fig S8Q–V). Inactivation of *daf-16* and *xbp-1* had no effect on mitochondrial stress-induced autophagy (Supplementary Fig S8W–Z). LGG-1 levels and LGG-1::GFP puncta accumulated in *egl-46* and *gfi-1* mutants (Fig 4I and J; Supplementary Fig S8A2). Transcription of *bec-1*, *epg-8*, *lgg-1,* and *atg-7* was upregulated in *egl-46*, *gfi-1*, and *E04A4.5* mutants and reduced by simultaneous loss of *atfs-1* activity (Supplementary Fig S8B2). Thus, mitochondrial stress activates autophagy through ATFS-1-mediated upregulation of autophagy genes.

The TGF-β, *lin-35*/Rb, ER stress, and mitochondrial stress pathways activate autophagy activity independent of HLH-30

The *C. elegans* TFEB homolog HLH-30 activates the expression of autophagy genes during starvation [23,24]. Suppression of the *rpl-43* mutant phenotype by ER stress, by mitochondrial stress, or by the loss of activity of *lin-35* and *sma-3* was not affected by simultaneous depletion of *hlh-30* (Supplementary Fig S9A-H). The transcription factor MXL-3 acts antagonistically to HLH-30 to repress the expression of lysosomal lipases [23]. Inactivation of *mxl-3* did not affect the accumulation of SQST-1::GFP aggregates in *rpl-43* mutants (Supplementary Fig S9I and J), indicating that autophagy activity was not elevated in the *mxl-3* mutant intestine. Thus, TGF-β, *lin-35*/Rb, ER stress, and mitochondrial stress signaling function in parallel to HLH-30 to control autophagy gene expression.

Here, we established the degradation of SQST-1 aggregates in the *rpl-43* mutant intestine as a genetic model system to investigate autophagy regulation. We demonstrated that autophagy activity is elevated by various stresses. ER stress and mitochondrial stress activate autophagy activity by transcriptional upregulation of autophagy genes in *C. elegans*. Components of the endocytic pathway, including the AP2 complex, the COG complex, and the ESCRT complex, were identified in our screen probably because their partial loss of function may not impair their normal function in the autophagy pathway [3], but impose a stress on the intestine which in turn activates autophagy.

In addition to these stress-induced gene inactivations, we found that the loss of activity of several developmental signaling pathways, including TGF-β, *lin-35*/Rb, *glp-1*, *daf-2*, mTOR, and LIN-45/MEK-2/MPK-1 MAPK signaling, promotes autophagy activity. TGF-β *lin-35*/Rb and *glp-1* signaling specify distinct biological processes by transcriptionally regulating distinct target genes and also transcriptionally promote autophagy activity [24]. Therefore, various developmental signaling factors integrate with the autophagy machinery during animal development.

Materials and Methods

See Supplementary Materials and Methods for strains used and additional protocols.

Identification, mapping, and cloning of *rpl-43*

bp399 was isolated in a genetic screen for mutants with ectopic accumulation of SQST-1::GFP aggregates. *bp399* was mapped between the polymorphic markers *pkp2118* (II: +21.2) and *pkp2113* (II: +22.9). Fosmids in this region were used for transformation rescue. Accumulation of SQST-1::GFP aggregates in *rpl-43*(*bp399*) animals was rescued by a transgene expressing the single gene *y48b6a.2* (including an approximately 1.5-kb promoter region, the entire ORF, and the approximately 1-kb 3′ UTR).

Preparation and induction of RNAi bacterial clones

The RNAi feeding library was purchased from Geneservice. The library contains bacterial clones expressing dsRNA designed to individually inactivate 16,749 genes (targeting about 87% of the predicted genes) [25]. RNAi bacterial clones were grown on LB agar plates supplemented with 100 mg/ml ampicillin and 30 mg/ml tetracycline and then inoculated into LB medium containing 50 mg/ml ampicillin and cultured for 6 h at 37°C. 300 μl of each bacterial culture was dispensed onto 10 cm NGM agar plates containing 5 mM IPTG. dsRNA transcription was induced overnight at 25°C. Synchronized L1 *sqst-1::gfp; rpl-43* animals were plated onto RNAi

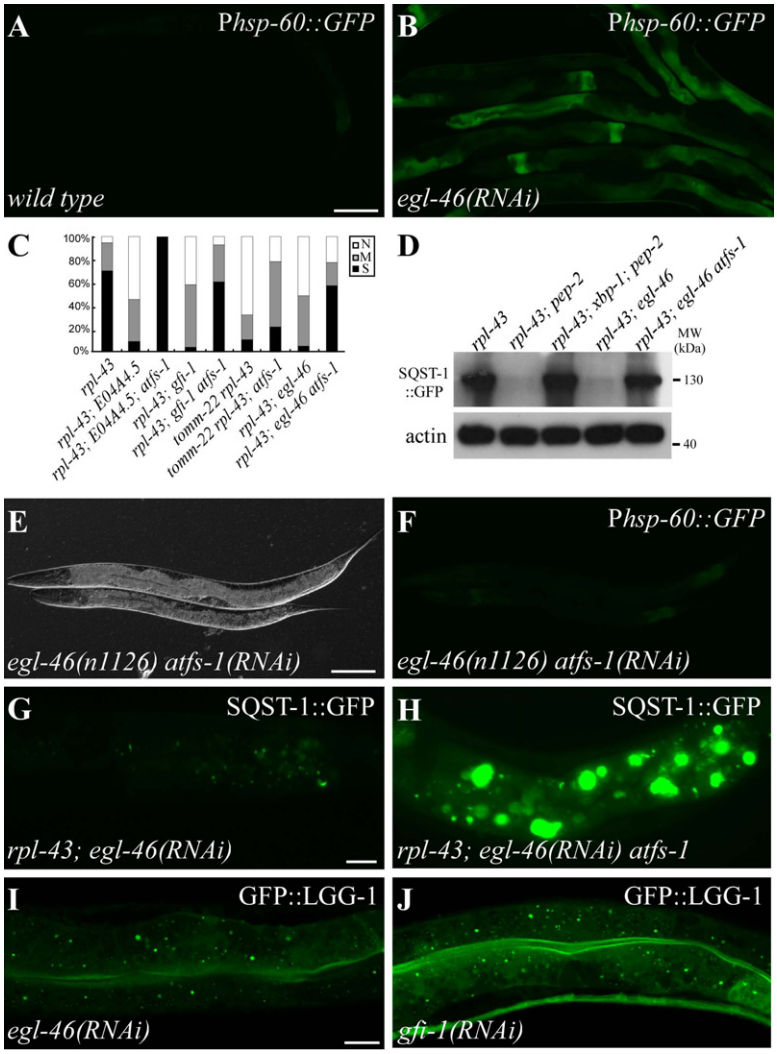

Figure 4. ATFS-1-mediated mitochondrial stress suppresses the *rpl-43* phenotype.

A P*hsp-60::GFP* is weakly expressed in wild-type animals.

B *egl-46*(*RNAi*) causes upregulation of P*hsp-60::GFP*.

C Percentage of indicated mutant animals with different levels of SQST-1::GFP aggregates. S: strong. M: medium. N: none. >30 animals were examined in each group.

D Levels of SQST-1::GFP in various genetic mutants. 200 young adult animals for each genotype were collected for analysis.

E, F Loss of function of *atfs-1* suppresses the upregulation of P*hsp-60::GFP* in *egl-46*(*n1126*) mutants. (E): DIC image of (F).

G, H The dramatic decrease in the number of SQST-1::GFP aggregates in the intestine in *rpl-43*(*bp399*); *egl-46*(*RNAi*) mutants (G) is restored by simultaneous loss of function of *atfs-1*(*gk3094*) (H).

I, J GFP::LGG-1 forms numerous puncta in the intestine in *egl-46*(*RNAi*) (I), *gfi-1*(*RNAi*) (J) animals.

Data information: Scale bars: 100 μm (A, B, E, F); 20 μm (G, H); 10 μm (I, J).

feeding plates with about 15 worms per plate and were grown at 20° C. The F1 progeny or arrested larvae or sterile adults were examined for expression of the *sqst-1::gfp* reporter.

Immunofluorescence staining

For worm immunofluorescence staining, animals were permeabilized by freeze-cracking and then fixed, blocked, and incubated with diluted antibody at room temperature for 2–4 h. The animals were then washed three times and incubated with rhodamine-conjugated or FITC-conjugated secondary antibody. Fluorescence was examined by a fluorescence microscope (Zeiss Axioplan 2 image) or a confocal microscope (Zeiss LSM 710 Meta plus Zeiss Axiovert zoom).

Statistical analysis

Data are shown as mean ± SD. Unpaired *t*-tests were performed for statistical analysis.

Supplementary information for this article is available online: http://embor.embopress.org

Acknowledgements
We are grateful to Dr. Isabel Hanson for editing work. This work was supported by the National Basic Research Program of China (2013CB910100, 2011CB910100) and also a grant from the NSFC (31225018) to H.Z. The research of Hong Zhang was supported in part by an International Early Career Scientist Grant from the Howard Hughes Medical Institute.

Author contributions
BG, XXH, PPZ, and HZ designed the experiments. BG, XXH, QQL, PPZ, LXQ, XBZ, JH, and BF performed the experiments. WRH and JHH performed bioinformatic analyses. BG, XXH, and HZ wrote the manuscript.

Conflict of interest
The authors declare that they have no conflict of interest.

References

1. Feng Y, He D, Yao Z, Klionsky DJ (2014) The machinery of macroautophagy. *Cell Res* 24: 24 – 41
2. Nakatogawa H, Suzuki K, Kamada Y, Ohsumi Y (2009) Dynamics and diversity in autophagy mechanisms: lessons from yeast. *Nat Rev Mol Cell Biol* 10: 458 – 467
3. Lamb CA, Yoshimori T, Tooze SA (2013) The autophagosome: origins unknown, biogenesis complex. *Nat Rev Mol Cell Biol* 14: 759 – 774
4. Lu Q, Wu F, Zhang H (2013) Aggrephagy: lessons from *C. elegans*. *Biochemical J* 452: 381 – 390
5. Itakura E, Kishi-Itakura C, Mizushima N (2012) The hairpin-type tail-anchored SNARE syntaxin 17 targets to autophagosomes for fusion with endosomes/lysosomes. *Cell* 151: 1256 – 1269
6. He C, Klionsky DJ (2009) Regulation mechanisms and signaling pathways of autophagy. *Annu Rev Genet* 43: 67 – 93
7. Sengupta S, Peterson TR, Sabatini DM (2010) Regulation of the mTOR complex 1 pathway by nutrients, growth factors, and stress. *Mol Cell* 40: 310 – 322
8. Russell RC, Yuan HX, Guan KL (2014) Autophagy regulation by nutrient signaling. *Cell Res* 24: 42 – 57
9. Lipinski MM, Hoffman G, Ng A, Zhou W, Py BF, Hsu E, Liu X, Eisenberg J, Liu J, Blenis J, et al (2010) A genome-wide siRNA screen reveals multiple mTORC1 independent signaling pathways regulating autophagy under normal nutritional conditions. *Dev Cell* 18: 1041 – 1052
10. Settembre C, Di Malta C, Polito VA, Garcia Arencibia M, Vetrini F, Erdin S, Erdin SU, Huynh T, Medina D, Colella P, et al (2011) TFEB links autophagy to lysosomal biogenesis. *Science* 332: 1429 – 1433
11. Chauhan S, Goodwin JG, Chauhan S, Manyam G, Wang J, Kamat AM, Boyd DD (2013) ZKSCAN3 is a master transcriptional repressor of autophagy. *Mol Cell* 50: 16 – 28
12. Tian Y, Li ZP, Hu WQ, Ren HY, Tian E, Zhao Y, Lu Q, Huang XX, Yang PG, Li X, et al (2010) *C. elegans* screen identifies autophagy genes specific to multicellular organisms. *Cell* 141: 1042 – 1055
13. Zhang YX, Yan LB, Zhou Z, Yang PG, Tian E, Zhang K, Zhao Y, Li ZP, Song B, Han JH, et al (2009) SEPA-1 mediates the specific recognition and degradation of P granule components by autophagy in *C. elegans*. *Cell* 136: 308 – 321
14. Lin L, Yang PG, Huang XX, Zhang H, Lu Q, Zhang H (2013) The scaffold protein EPG-7 links cargo-receptor complexes with the autophagic assembly machinery. *J Cell Biol* 201: 113 – 129
15. Zhong W, Sternberg PW (2006) Genome-wide prediction of *C. elegans* genetic interactions. *Science* 311: 1481 – 1484
16. Lee I, Lehner B, Crombie C, Wong W, Fraser AG, Marcotte EM (2008) A single gene network accurately predicts phenotypic effects of gene perturbation in *Caenorhabditis elegans*. *Nat Genet* 40: 181 – 188
17. Savage-Dunn C (2005) TGF-beta signaling. *WormBook* Sep 9: 1 – 12
18. Wu X, Shi Z, Cui M, Han M, Ruvkun G (2012) Repression of germline RNAi pathways in somatic cells by retinoblastoma pathway chromatin complexes. *PLoS Genet* 8: e1002542
19. Meléndez A, Tallóczy Z, Seaman M, Eskelinen EL, Hall DH, Levine B (2003) Autophagy genes are essential for dauer development and life-span extension in *C. elegans*. *Science* 301: 1387 – 1391
20. Jia K, Chen D, Riddle DL (2004) The TOR pathway interacts with the insulin signaling pathway to regulate *C. elegans* larval development, metabolism and life span. *Development* 131: 3897 – 3906
21. Cao SS, Kaufman RJ (2012) Unfolded protein response. *Curr Biol* 22: R622 – R626
22. Pellegrino MW, Nargund AM, Haynes CM (2013) Signaling the mitochondrial unfolded protein response. *Biochim Biophys Acta* 1833: 410 – 416
23. O'Rourke EJ, Ruvkun G (2013) MXL-3 and HLH-30 transcriptionally link lipolysis and autophagy to nutrient availability. *Nat Cell Biol* 15: 668 – 676
24. Lapierre LR, De Magalhaes Filho CD, McQuary PR, Chu CC, Visvikis O, Chang JT, Gelino S, Ong B, Davis AE, Irazoqui JE, et al (2013) The TFEB orthologue HLH-30 regulates autophagy and modulates longevity in *Caenorhabditis elegans*. *Nat Commun* 4: 2267
25. Kamath RS, Ahringer J (2003) Genome-wide RNAi screening in *Caenorhabditis elegans*. *Methods* 30: 313 – 321